Journal of Cranio-Maxillo-Facial Surgery 47 (2019) 341–348

Contents lists available at ScienceDirect

Journal of Cranio-Maxillo-Facial Surgery

journal homepage: www.jcmfs.com

A polycaprolactone-β-tricalcium phosphate–heparan sulphate device for cranioplasty

Bach Quang Le [a], Bina Rai [a, 1], Zophia Xue Hui Lim [a], Tuan Chun Tan [a], Tingxuan Lin [a], Jaslyn Jie Lin Lee [a], Sadasivam Murali [a], Swee Hin Teoh [b], Victor Nurcombe [a], Simon McKenzie Cool [a, c, *]

[a] Institute of Medical Biology, Agency for Science, Technology and Research (A*STAR), 8A Biomedical Grove, #06-06 Immunos, Singapore 138648
[b] Centre for Bone Tissue Engineering, School of Chemical and Biomedical Engineering, Lee Kong Chian School of Medicine, Nanyang Technological University Singapore, 62 Nanyang Drive, 637459, Singapore
[c] Department of Orthopaedic Surgery, Yong Loo Lin School of Medicine, National University of Singapore, Singapore 119288

ARTICLE INFO

Article history:
Paper received 15 August 2018
Accepted 12 November 2018
Available online 16 November 2018

Keywords:
Calvarial defect
Glycosaminoglycans
Heparan sulphate
BMP-2
PCL-TCP

ABSTRACT

Background: Cranioplasty is a surgical procedure used to treat a bone defect or deformity in the skull. To date, there is little consensus on the standard-of-care for graft materials used in such a procedure. Graft materials must have sufficient mechanical strength to protect the underlying brain as well as the ability to integrate and support new bone growth. Also, the ideal graft material should be individually customized to the contours of the defect to ensure a suitable aesthetic outcome for the patient.
Purpose: Customized 3D-printed scaffolds comprising of polycaprolactone-β-tricalcium phosphate (PCL-TCP) have been developed with mechanical properties suitable for cranioplasty. Osteostimulation of PCL-TCP was enhanced through the addition of a bone matrix-mimicking heparan sulphate glycosaminoglycan (HS3) with increased affinity for bone morphogenetic protein-2 (BMP-2). Efficacy of this PCL-TCP/HS3 combination device was assessed in a rat critical-sized calvarial defect model.
Method: Critical-sized defects (5 mm) were created in both parietal bones of 19 Sprague Dawley rats (Male, 450–550 g). Each cranial defect was randomly assigned to 1 of 4 treatment groups: (1) A control group consisting of PCL-TCP/Fibrin alone (n = 5); (2) PCL-TCP/Fibrin-HSft (30 μg) (n = 6) (HSft is the flow-through during HS3 isolation that has reduced affinity for BMP-2); (3) PCL-TCP/Fibrin-HS3 (5 μg) (n = 6); (4) PCL-TCP/Fibrin-HS3 (30 μg) (n = 6). Scaffold integration and bone formation was evaluated 12-weeks post implantation by μCT and histology.
Results: Treatment with PCL-TCP/Fibrin alone (control) resulted in 23.7% ± 1.55% (BV/TV) of the calvarial defect being filled with new bone, a result similar to treatment with PCL-TCP/Fibrin scaffolds containing either HSft or HS3 (5 μg). At increased amounts of HS3 (30 μg), enhanced bone formation was evident (BV/TV = 38.6% ± 9.38%), a result 1.6-fold higher than control. Further assessment by 2D μCT and histology confirmed the presence of enhanced bone formation and scaffold integration with surrounding host bone only when scaffolds contained sufficient bone matrix-mimicking HS3.
Conclusion: Enhancing the biomimicry of devices using a heparan sulphate with increased affinity to BMP-2 can serve to improve the performance of PCL-TCP scaffolds and provides a suitable treatment for cranioplasty.

1. Introduction

Large bone defects in the skull following trauma or brain surgery, such as trepanation, must be treated promptly to restore the protective and cosmetic function of the skull. Such cranioplasty procedures date back thousands of years, yet they still remain a challenge for clinicians, despite extensive research and advances in

* Corresponding author. Institute of Medical Biology, Agency for Science, Technology and Research (A*STAR), 8A Biomedical Grove, #06-06 Immunos, Singapore 138648. Fax: +65 6779 1117.
E-mail address: simon.cool@imb.a-star.edu.sg (S.M. Cool).
[1] Present address: Science and Maths Cluster, Singapore University of Technology & Design (SUTD), 8 Somapah Road, Singapore 487372.

https://doi.org/10.1016/j.jcms.2018.11.013
1010-5182/

our understanding of the human body and bone biology (Donati et al., 2007; Feroze et al., 2015). The current reported complication rate ranges from 16% to 40% and the general reoperation rate is about 25% (Feroze et al., 2015).

First reported in the 1900s, autologous bone graft (ABG) is still considered the "gold standard" for management of bone defects and nonunion (Biasibetti et al., 2005; Albee, 2007; Pape et al., 2010; Sakkas et al., 2017). However, high failure rates while using ABG for cranioplasty can occur due to bone resorption and infection that necessitate additional surgeries (Lee et al. 2013, 2014; Martin et al., 2014; Krishnan et al., 2016; Park et al., 2017). Also, for calvarial reconstruction following craniectomy, the patient's skull flap (ABG) is typically preserved for later use by either cryopreservation or subcutaneous implantation under the patient's skin, a process that further reduces the effectiveness of such a grafting procedure (Morina et al., 2011; Sundseth et al., 2014). In such cases, harvesting fresh ABG from another anatomical location causes yet another morbidity burden to suffering patients. Collectively, these adverse events highlight the need for ABG substitutes that are efficacious for the repair of calvarial defects. However, there is little consensus on the most suitable graft material for cranioplasty (Khader and Towler, 2016; Zanotti et al., 2016).

The ideal cranioplasty graft must at least have the following properties: (a) It must provide immediate and long-term mechanical protection for the underlying brain (until the host bone fully regenerates), (b) It must recreate the skull contour for cosmetic purposes, and (c) The graft must either be replaced by host bone at the same rate, or remain a prosthesis without causing complication and inconvenience to the patient's life (Aydin et al., 2011; Khader and Towler, 2016).

One particular material, bioresorbable polycaprolactone–tricalcium phosphate (PCL–TCP), can be manufactured into scaffolds that fulfil these requirements and has been shown to be effective in a range of dental and bone tissue-engineering applications (Zein et al., 2002; Rai et al., 2007a, 2007b; Yeo et al. 2008, 2010a, 2010b, 2012; Abbah et al., 2011; Li et al., 2014). PCL has been extensively tested *in vitro* and *in vivo* as a scaffolding material for bone and cartilage tissue engineering, resulting in a number of FDA-approved devices (Motamedian et al., 2015; Shim et al., 2017). PCL alone is a biocompatible material with many advantages, including that its flexible, biodegradable and bioresorbable properties. TCP is a known osteoconductive material, plus TCP can bind proteins including bone morphogenetic proteins (BMPs) (Maus et al., 2008). Furthermore scaffolds containing both PCL and TCP have been shown to support the delivery of BMP-2 at bone defect sites (Rai et al. 2004, 2005). Also, TCP helps to accelerate the degradation of PCL-based scaffolds when compared to PCL alone (Yeo et al., 2008, Yeo et al., 2010a, 2010b).

Utilizing fused deposition modelling, PCL–TCP scaffolds can be printed to any customized shape, allowing seamless integration into the skull defect and the aesthetic contours of the cranium. Moreover, a suitable mechanical strength can be achieved by adjusting the chemical composition and fabricating pattern, so producing scaffolds with tunable load-bearing properties for use in long bone, spine, and craniofacial defects (Zein et al., 2002). Furthermore, by incorporating autologous cells or extracellular matrix (ECM) mimicking substances into the pores of the PCL–TCP scaffolds, we have demonstrated significant improvement in graft integration and osteogenesis (Rai et al., 2007a, 2007b; Abbah et al., 2011).

Concomitantly, we have developed a heparan sulphate (HS) variant that mimics HS in bone tissue and avidly binds and supports the actions of the potent osteogenic factor BMP-2 (termed HS3) (Murali et al., 2013). We have shown that HS3 can be added to scaffolds to support the body's natural endogenous bone healing processes (Ling et al., 2006; Manton et al., 2006; Jackson et al., 2007; Murali et al., 2009; Ling et al., 2010; Bramono et al., 2012; Murali et al., 2013; Rai et al., 2015, Bhakta et al., 2017), which highlights the important role of heparan sulphate in modulating growth factor-mediated tissue developmental and repair, including those of bone (Cool and Nurcombe, 2006; Song et al., 2006). In these studies, we exemplified the ability of HS3 to support endogenous bone healing cascades when combined with a range of clinically-approved materials, including collagen (Murali et al., 2013) and β-TCP/carboxymethyl cellulose (CMC) (Rai et al., 2015) devices. We have since developed an HS3-silane-modified PCL–TCP/collagen device as a scaffold for the delivery of BMP-2 for spinal fusion applications (Bhakta et al., 2017). Furthermore, HS-like materials have also enhanced tissue regeneration when functionalized to materials (Albo et al., 1996; Lafont et al., 1998; Escartin et al., 2003; Lee et al., 2017), providing additional support for the use of glycosaminoglycan-based strategies in regenerative medicine.

Here we report on the development of a PCL–TCP/fibrin–HS3 device for cranioplasty. Using a rat calvarial defect model, we hypothesized that PCL–TCP/fibrin devices incorporating the bone matrix-mimicking heparan sulphate glycosaminoglycan, HS3, could help to regenerate more new bone than native PCL–TCP/fibrin scaffolds.

2. Materials and methods

2.1. Materials

All reagents and chemicals were purchased from Sigma (St. Louis, MO, USA) unless otherwise stated. Heparan sulphate (HS3) was isolated and prepared as previously described (Murali et al., 2013). Scaffolds of PCL-β-TCP (PCL–TCP) were from Osteopore International Pte Ltd, Singapore.

2.2. Experimental design

For this study, we utilized a bilateral critical-sized (5-mm) rat calvarial defect model with a 12-week healing timepoint that is well-established in the literature (Bosch et al., 1998; Alhag et al., 2012; He et al., 2014; Samsonraj et al., 2017). A critical-sized calvarial defect (5 mm) was created in each parietal bone of nineteen 12–13-week-old male Sprague Dawley rats (InVivos, Singapore) weighing 450–550 g. Of the 38 defects, 23 were used in this study, and the remaining 15 defects were utilized in a parallel study. Each defect was randomly treated with one of four experimental groups: 1) PCL–TCP/Fibrin alone ($n = 5$), 2) PCL–TCP/Fibrin–HSft (30 μg) – the low BMP-2 binding HS variant (Murali et al., 2013) ($n = 6$), 3) PCL–TCP/Fibrin–HS3 (5 μg) – the high BMP-2 binding HS variant (Murali et al., 2013) ($n = 6$), and 4) PCL–TCP/Fibrin–HS3 (30 μg) ($n = 6$). Power analysis was performed using G*Power (V3.1.9), with effective size calculated using data from two similar studies (Colombier et al., 1999; Alhag et al., 2012). In accordance with IACUC principles for reduction of animal usage, treatment groups were randomized across the animals, with each animal receiving more than one treatment.

At 12 weeks post-treatment, animals were sacrificed by CO_2 and the parietal bones containing the defects harvested and processed for micro-Computed Tomography (μCT) and histological analysis (Table 1) as previously reported by our group (Murali et al., 2013; Rai et al., 2015).

2.3. Scaffold preparation

The scaffolds were purchased directly from Osteopore International, Singapore. Scaffolds were fabricated in blocks measuring

Table 1
Experimental design.

Sample #	Rat ID	Treatment	Time point	μCT Analysis	Paraffin histology
1	B1L2R2L	PCL–TCP/fibrin	12 week	✓	✓
2	B1R2R	PCL–TCP/fibrin	12 week	✓	–
3	B1NPL	PCL–TCP/fibrin	12 week	PV	–
4	B2L2R2L	PCL–TCP/fibrin	12 week	✓	–
5	B2NPL	PCL–TCP/fibrin	12 week	✓	✓
6	B1L1R2R	PCL–TCP/fibrin–HSft (30 μg)	12 week	DPP	–
7	B1L3R1L	PCL–TCP/fibrin–HSft (30 μg)	12 week	✓	✓
8	B1R1L	PCL–TCP/fibrin–HSft (30 μg)	12 week	✓	✓
9	B2L1R1R	PCL–TCP/fibrin–HSft (30 μg)	12 week	✓	✓
10	B2L1R2R	PCL–TCP/fibrin–HSft (30 μg)	12 week	✓	–
11	B2R1L	PCL–TCP/fibrin–HSft (30 μg)	12 week	✓	–
12	B1L1R	PCL–TCP/fibrin–HS3 (5 μg)	12 week	PV	–
13	B1L1R1L	PCL–TCP/fibrin–HS3 (5 μg)	12 week	✓	–
14	B1L3R1R	PCL–TCP/fibrin–HS3 (5 μg)	12 week	✓	✓
15	B2L1R	PCL–TCP/fibrin–HS3 (5 μg)	12 week	✓	✓
16	B2L1R1L	PCL–TCP/fibrin–HS3 (5 μg)	12 week	✓	✓
17	B2L1R3L	PCL–TCP/fibrin–HS3 (5 μg)	12 week	✓	–
18	B1L1L	PCL–TCP/fibrin–HS3 (30 μg)	12 week	✓	–
19	B1R3L	PCL–TCP/fibrin–HS3 (30 μg)	12 week	✓	✓
20	B2L1L	PCL–TCP/fibrin–HS3 (30 μg)	12 week	✓	✓
21	B2L2L	PCL–TCP/fibrin–HS3 (30 μg)	12 week	✓	–
22	B2L3R2L	PCL–TCP/fibrin–HS3 (30 μg)	12 week	✓	–
23	B2L3R3L	PCL–TCP/fibrin–HS3 (30 μg)	12 week	✓	✓

(✓) Analysis performed.
(–) No analysis performed.
(DPP) Damaged post-processing.
(PV) Protocol violation.

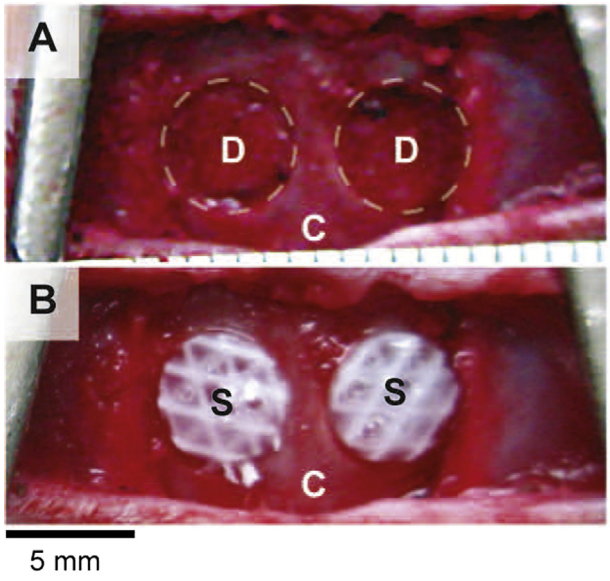

Fig. 1. Representative images showing the rat critical-sized calvarial defect model. (A) Two full-thickness defects of diameter 5 mm were trephined at the center of each parietal bone. (B) Two PCL–TCP scaffolds of diameter 5 mm, pre-loaded with fibrin and HS test articles were press-fit into the defects. (D = defect; S = scaffold; C = calvaria). (Scale bar = 5 mm).

50 × 50 × 1 mm^3 with PCL–TCP (PCL 80%–TCP 20%, filament diameter ~250 μm), a lay-down pattern of 0/90, and a porosity of 70%. The scaffolds were then cut into 5 mm diameter discs using a biopsy punch. The scaffold discs were then surface treated with 5 M NaOH for 3 h at 37 °C, then washed with PBS six times, and dried in a laminar flow hood. They were then sterilized in 70% ethanol for 24 h and rinsed twice in PBS before being used for experiments. The HS variants HSft (30 μg) and HS3 (5 μg and 30 μg) were dissolved in PBS (15 μl) and loaded into the pores of each scaffold with Fibrin (10 μl) (*TISSEEL* kit; Baxter AG), and kept in sterile conditions at room temperature 2 h prior to surgery in a manner similar to our previous study using another HS variant (Woodruff et al., 2007).

2.4. Surgical procedures

Surgical procedures were performed as previously reported by our group (Sawyer et al., 2009) with approval from the Institutional Animal Care and Use Committee, A*STAR Singapore, (IACUC number 080379). Rats were anaesthetized with isoflurane and a midline calvarial incision made and the periosteum removed. A full-thickness 5 mm diameter defect was created in the center of each parietal bone using a slow-speed dental drill (Strong 209A SAESHIN, Korea) under saline irrigation. Scaffold treatments were then implanted into the defects (Fig. 1). Subcutaneous administration of prophylactic antibiotics (Baytril, 10 mg/kg) and analgesics (Butorphanol, 1 mg/kg) were delivered for 3 days post-surgery, and the animals allowed to recover for 12 weeks post-surgery.

2.5. Micro-computed tomography (μCT) analysis

Harvested samples were scanned using a Skyscan 1076 (Bruker, Belgium) μCT scanner at a resolution of 35 μm, voltage of 100 kV, and current of 100 μA. Defects were then reconstructed and the extent of bone healing determined using the manufacturer's software (NRecon-v1.6.9.18, Dataviewer-v1.5.4.0, CTAn-v1.14.11.0, Bruker, Belgium). For analysis, a cylindrical region of interest (ROI) measuring 5 mm in diameter and 1 mm in thickness was positioned in the defect and the volume of newly formed bone within this ROI (%BV/TV) determined using the CTAn software with bone threshold values between 50 and 255 (arbitrary grayscale unit). The threshold was determined based on visualization of bone morphology and the same threshold (50–255) was rigorously applied to all samples throughout all analyses. Representative 3D-reconstructions and 2D slices using CTAn and Dataviewer software were used to assess the structure and distribution of bone within the defects.

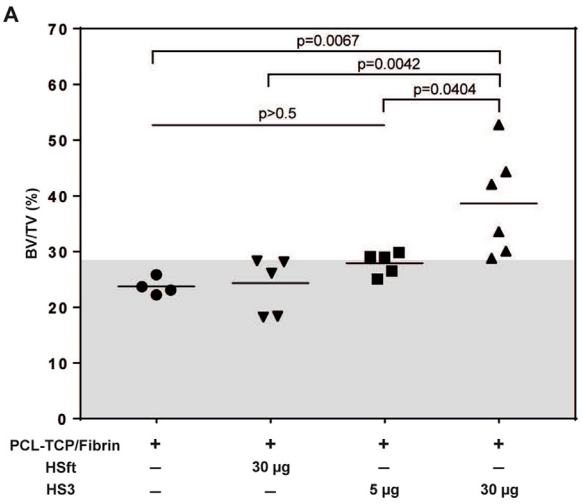

B

BV/TV(%)	PCL-TCP/ Fibrin	PCL-TCP/ Fibrin + HSft (30µg)	PCL-TCP/ Fibrin + HS3 (5µg)	PCL-TCP/ Fibrin + HS3 (30µg)
0 - 28.3	4 (100%)	5 (100%)	2 (40%)	0 (0%)
28.4 - 60	0 (0%)	0 (0%)	3 (60%)	6 (100%)
Min	22.3	18.2	25.1	28.8
Max	25.9	28.3	29.8	52.8
Mean	23.7	23.8	27.9	38.6
Mean fold change rel. to PCL-TCP/Fibrin	1.0	1.0	1.2	1.6
Median	23.4	26.1	29	37.9
Standard deviation	1.6	5.1	2.0	9.4
Coefficient of variation	6.5	21.5	7.2	24.3

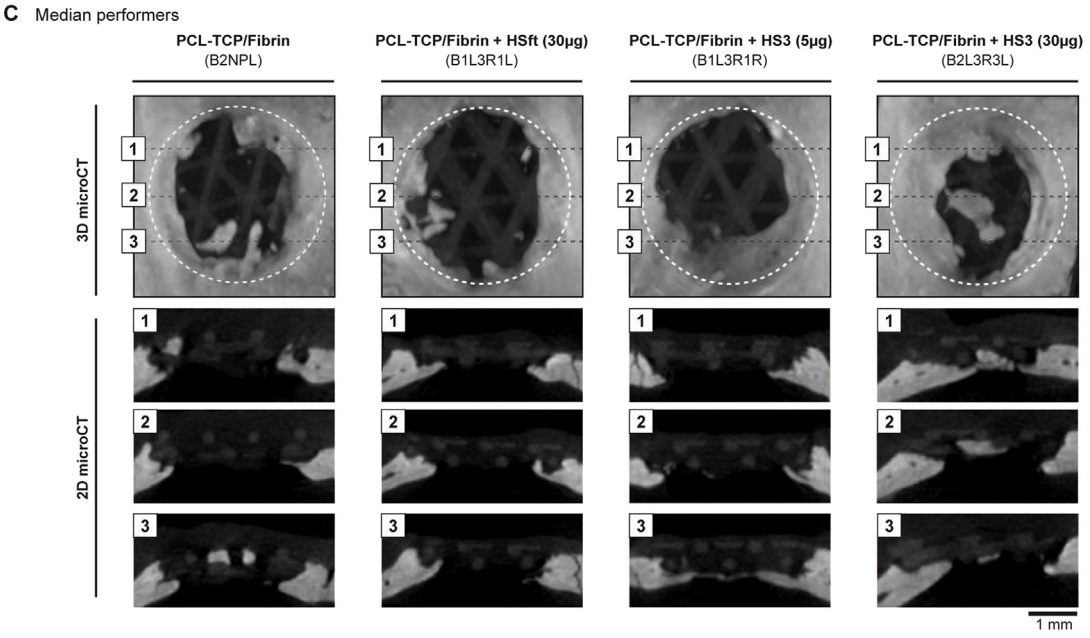

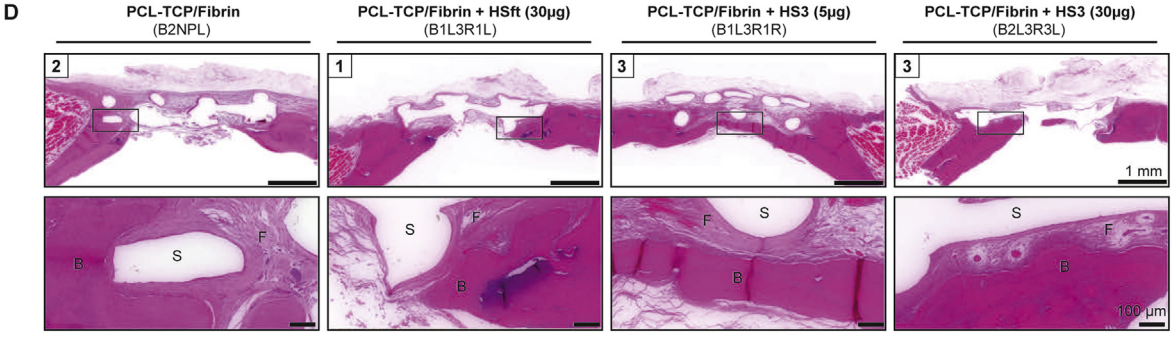

Fig. 2. Analysis by µCT and histology of defects 12-weeks post-implantation. (A) Percent bone volume in defects (BV/TV%) determined by CTAn software. Shading represents values above and below the highest BV/TV% value for PCL–TCP/Fibrin–HSft (30 µg). Adjusted p values of the ANOVA test with Tukey post-test were reported. (B) Table summarising the number of data points in each shading zone (BV/TV% value from 0 to 28.3 and from 28.4 to 60) as well as descriptive statistics of BV/TV% data including the min, max, mean, mean fold change relative to PCL–TCP/Fibrin, median, and standard deviation of each group. (C) 3D-reconstructed µCT images (top-down view) generated by CTAn software and 2D µCT slides taken coronally at the front-1, middle-2 and back-3 of the defect of the median performers (according to BV/TV% analysis). (Scale bar = 1 mm). (D) Histomicrographs of the median performers (same as above) taken from paraffin sections stained with Haematoxylin & Eosin at 2 magnifications (small box indicates the magnified region; B = bone; S = scaffold; F = fibrous tissue). The approximate position the histological sections were taken from was estimated (small number at top left of each image) by matching features in the images to their corresponding 2D µCT sections above.

2.6. Histology

After μCT scanning, parietal bones were fixed, decalcified, paraffin embedded, and sectioned as previously described (Sawyer et al., 2009; Rai et al., 2015). Sections were taken in the coronal plane through the middle of the defect and stained with Haematoxylin & Eosin and imaged using the Zeiss Axio Imager or the Metasystems Slidescanner.

2.7. Statistical analyses

Statistical analyses were performed using ANOVA (GraphPad Prism v7) with Tukey post-hoc testing was selected to correct for unequal N. The adjusted p values were reported, and a p value <0.05 was considered significant.

3. Results

3.1. Animal surgery

All rats recovered well after the surgery with good initial placement of the various scaffold treatments (Fig. 1). However, at the endpoint (12 weeks), two samples (PCL–TCP/Fibrin alone and PCL–TCP/Fibrin–HS3 (5 μg)) had dislodged from the defect site (protocol violation – PV) and were removed from the study (Supp. Fig. 3). Also,

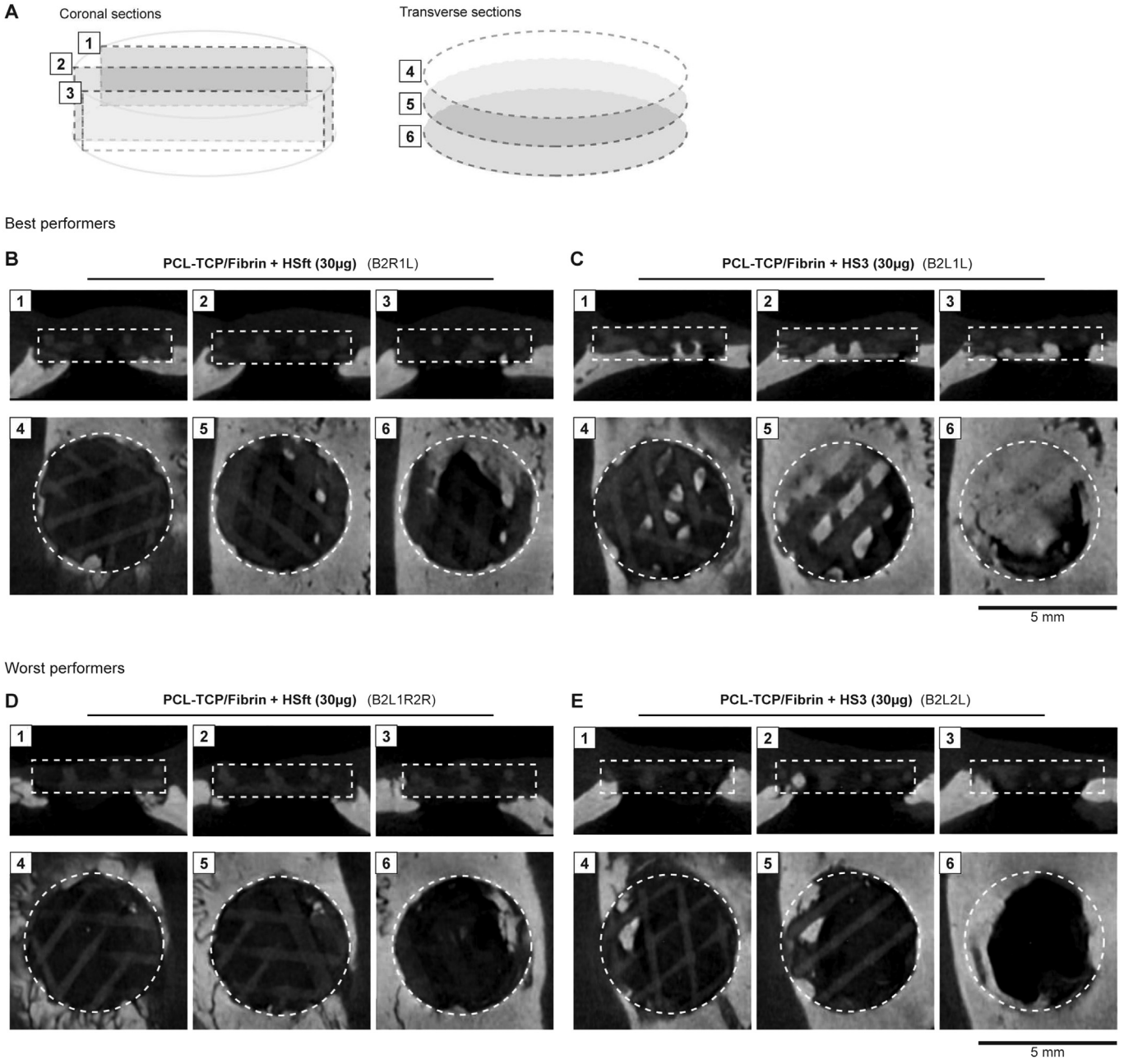

Fig. 3. 2D μCT slices of the best and worst performers (according to BV/TV% analysis) from the PCL–TCP/Fibrin–HSft (30 μg) and PCL–TCL/Fibrin–HS3 (30 μg) treatment groups. (A) Schematic diagram showing the positions of the cross-sections taken through the defect site. (B & C) 2D μCT slices of the best performers in the aforementioned groups. (D & E) 2D μCT slices of the worst performers in the aforementioned groups. (Scale bar = 5 mm).

one sample from the PCL–TCP/Fibrin–HSft group was damaged post-processing (DPP) and was deleted from the study (Table 1).

3.2. Volumetric assessment of bone formation in scaffolds by μCT

To quantify the amount of new bone formed by each treatment group (BV/TV%), μCT analysis was performed on the harvested defects (Fig. 2A & B). Whenever PCL–TCP/Fibrin scaffolds contained an appropriate amount of the bone matrix-mimicking glycosaminoglycan HS3 (30 μg), a significant increase in new bone formation (BV/TV = 38.6%) was observed (PCL–TCP/Fibrin–HS3 (30 μg) vs. PCL–TCP/Fibrin: $p = 0.0067$; vs. PCL–TCP/Fibrin–HSft: $p = 0.0042$ and vs. PCL–TCP/Fibrin–HS3 (5 μg): $p = 0.0404$). By comparison, treatment with PCL–TCP/Fibrin alone resulted in a BV/TV of 23.7%, a result 1.6-fold lower than when HS3 was added. Notably, adding a heparan sulphate glycosaminoglycan with low affinity for BMP-2 (HSft), provided no benefit over PCL–TCP/Fibrin alone (BV/TV = 23.8%). Also, lowering the amount of HS3 to 5 μg produced a result similar to both PCL–TCP/Fibrin alone (BV/TV = 27.9%) and PCL–TCP/Fibrin–HSft.

To further assess the benefits of using an HS variant that mimics HS from the bone microenvironment (HS3), we compared the spread of BV/TV data between the various treatment groups. For comparison purposes, BV/TV values above and below the highest value for PCL–TCP/Fibrin–HSft (28.3%) were shaded and the results in the two regions enumerated (Fig. 2A & B). Data show that 100% of defects treated with PCL–TCP/Fibrin–HS3 (30 μg) and 60% of defects treated with PCL–TCP/Fibrin–HS3 (5 μg) out-performed (more new bone formation) the best result for both PCL–TCP/Fibrin and PCL–TCP/Fibrin–HSft (Fig. 2B).

3.3. Morphological assessment of bone bridging in defect by μCT and histology

To evaluate the form and structure of new bone in the defect sites, multiple 3D images and 2D slices were analysed from reconstructed μCT scans (Figs. 2C, 3, and Supp. Figs. 1 & 2). Fig. 2C shows representative μCT images of median performers (based on BV/TV values) for each treatment group. The 3D reconstructions show that treatment with PCL–TCP/Fibrin–HS3 (30 μg), increased the amount of bone bridging across the defect when compared to the other treatments groups. Also, in most cases, 2D μCT slices clearly show that PCL–TCP/Fibrin–HS3 (30 μg) treatment resulted in bone infiltrating the outer edges of the scaffold, indicating enhanced integration between the host bone and the PCL–TCP/Fibrin–HS3 scaffold. Notably, bone infiltrating into the middle of the PCL–TCP/Fibrin scaffold (in all 3 coronal sections) was only observed with PCL–TCP/Fibrin–HS3 (30 μg) treatment (Figs. 2C, 3, and Supp. Figs. 1 & 2).

Having observed that HS3 (30 μg) enhanced the therapeutic performance of PCL–TCP/Fibrin scaffolds, we sought to understand whether this effect was related to the BMP-2-binding affinity of the HS variant used. Because HSft has a lower BMP-2-binding affinity than HS3, we compared the bone-healing efficacy of these two HS variants (using the same amount of each HS variant) when added to PCL–TCP/Fibrin scaffolds (Fig. 3). Analysis of 2D μCT slices from multiple levels (in both the coronal and transverse plane) clearly showed that even the best outcome from the PCL–TCP/Fibrin–HSft group failed to regenerate bone within the defect space, and only a small amount of new bone was present in the floor of the calvarial defect (Fig. 3B). In comparison, the best performer of the PCL–TCP/Fibrin–HS3 (30 μg) treatment resulted in near-complete filling of the defect, with new bone present throughout the scaffold (Fig. 3C). Furthermore, when comparing the worst outcomes between the two treatments (PCL–TCP/Fibrin–HSft versus PCL–TCP/Fibrin–HS3 (30 μg)) it is clearly evident that addition of HS3, despite the low amount of new bone, still resulted in a good integration between the scaffold and host bone (Fig. 3E) that was absent in the PCL–TCP/Fibrin–HSft treatment group (Fig. 3D).

In all cases, histological assessment using coronal sections matched to reconstructed 2D μCT slices acted to confirm the μCT findings (Fig. 2D and Supp. Figs. 1 & 2). Structures that were visualized as bone at the predefined μCT threshold were confirmed to be bone tissue under H&E staining. It was apparent that the PCL–TCP scaffolds struts dissolved from the slides during histology processing, leaving white spaces in the tissue sections. However, it is clear that the pores of the scaffolds were always filled with fibrous tissue if bone was not present. Overall, irrespective of treatment, there was some bone ingrowth from the host into the sides of the scaffolds, which helped to secure the scaffolds within the defect. However, bone ingrowth that reached the centre of the scaffolds was only seen in the PCL–TCP/Fibrin–HS3 (30 μg) treatment group (Figs. 2C, D, 3C and Supp. Fig. 2B).

4. Discussion

The reconstruction of cranial defects serves to restore both aesthetic and protective functions. Numerous biomaterials have been evaluated as alternatives to bone grafting for these cranioplasty procedures, with mixed success. Our group has previously shown that the addition of recombinant human BMP-2 (rhBMP-2) to PCL–TCP/collagen devices greatly enhances their bone healing performance as press-fit devices for cranioplasty (Sawyer et al., 2009). However, the off-label use of recombinant proteins for craniofacial reconstructions has been associated with significant adverse events in up to 30% of patients (Shah et al., 2008; Alonso et al., 2010; Herford et al., 2011). Instead, we sought to harness the osteostimulatory activity of endogenous factors like BMP-2 through the addition of a BMP-2-binding heparan sulphate glycosaminoglycan variant (HS3). We have previously demonstrated that both collagen-HS3 and β -TCP/carboxymethylcellulose-HS3 devices are efficacious for long bone healing (Murali et al., 2013; Rai et al., 2015), suggesting HS3 is a likely candidate to improve the osteostimulatory properties of PCL–TCP/Fibrin scaffolds. Also, previous studies have shown that HS-functionalized scaffolds are efficacious for bone healing applications. Notably, Yang et al. showed that heparin-conjugated fibrin was able to sustain the osteoinductive effects of exogenously added BMP-2 through a heparin–protein interaction that resulted in enhanced bone regeneration (Yang et al., 2012). In parallel studies, our group has shown that fibrin–HS is efficacious for calvarial bone healing in the absence of exogenously added BMP-2 (Woodruff et al., 2007), highlighting the ability of devices containing HS to enhance osteostimulation and bone regeneration. In both studies, fibrin gel was utilized as a carrier for the bioadditives to mimic the release of growth factors from the blood clot during a natural healing process.

In the current study, fibrin–HS3 complexes were added to PCL–TCP scaffolds and used for the treatment of critical-sized rat calvarial defects. Here, we reasoned that PCL–TCP scaffolds would provide the mechanical support and osteoconductive surface to support bone regeneration, and that the addition of fibrin–HS3 would help to sequester and then stabilize endogenously produced growth factors like BMP-2, so further enhancing endogenous bone-stimulating signals from the bone defect. When PCL–TCP/Fibrin–HS3 (30 μg) was used to treat calvarial defects, increased amounts of new bone were observed within the injury site compared to all other treatments. Notably, the addition of a low BMP-2 affinity HS variant (HSft), resulted in minimal defect filling. We posit that PCL–TCP/fibrin–HS3 scaffolds are capable of

sequestering increased amounts of BMP-2 compared to PCL–TCP/fibrin–HSft or PCL–TCP/fibrin scaffolds. This is likely because HS3 is isolated by affinity chromatography using the heparin-binding domain of BMP-2 as the affinity ligand, whereas HSft represents the flow through HS material that has lower affinity for BMP-2 (Murali et al., 2013). Moreover, HSft-BMP-2 complexes do not increase the osteogenic effects of BMP-2, whereas HS3-BMP-2 significantly increases BMP-2-mediated osteogenesis; collagen/HSft devices are less efficacious for bone healing compared to collagen/HS3 (Murali et al., 2013). Our future studies are aimed at strategies to increase the bone mineral density and mechanical performance of these implants. Of note, sometimes we observed scaffold dislocation from the defect sites (2 cases in this study, in PCL–TCP/fibrin and PCL–TCP/fibrin–HS3–5 μg group) in the treatment that fails to regenerate bone in the defects. Thus, the speed at which new bone is formed within the scaffolds could play an important role in maintaining scaffold stability, which in turn may result in a better overall bone healing process. As such, developing combination devices that more closely mimic native tissues (like PCL–TCP/Fibrin–HS3) represents a therapeutic strategy that is both valid and effective.

5. Conclusion

Overall, we have demonstrated that an appropriate dose of HS3 enhanced the bone healing efficacy of the PCL–TCP/fibrin scaffolds in a rat calvarial defect model. This combinational device thus presents as a promising therapeutic option for the management of bone regeneration in cranioplasty.

Conflict of interest

The authors declare no conflict of interest.

Acknowledgements

The authors acknowledge funding support from the Institute of Medical Biology, Agency for Science, Technology and Research (A*STAR), Singapore.

Appendix A. Supplementary data

Supplementary data to this article can be found online at https://doi.org/10.1016/j.jcms.2018.11.013.

References

Abbah SA, Lam CX, Ramruttun KA, Goh JC, Wong HK: Autogenous bone marrow stromal cell sheets-loaded mPCL/TCP scaffolds induced osteogenesis in a porcine model of spinal interbody fusion. Tissue Eng A 17(5–6): 809–817, 2011
Albee FH: Transplantation of a portion of the tibia into the spine for Pott's disease: a preliminary report 1911. Clin Orthop Relat Res 460: 14–16, 2007
Albo D, Long C, Jhala N, Atkinson B, Granick MS, Wang T, et al: Modulation of cranial bone healing with a heparin-like dextran derivative. J Craniofac Surg 7(1): 19–22, 1996
Alhag M, Farrell E, Toner M, Lee TC, O'Brien FJ, Claffey N: Evaluation of the ability of collagen-glycosaminoglycan scaffolds with or without mesenchymal stem cells to heal bone defects in Wistar rats. Oral Maxillofac Surg 16(1): 47–55, 2012
Alonso N, Tanikawa DY, Freitas Rda S, Canan Jr L, Ozawa TO, Rocha DL: Evaluation of maxillary alveolar reconstruction using a resorbable collagen sponge with recombinant human bone morphogenetic protein-2 in cleft lip and palate patients. Tissue Eng C Methods 16(5): 1183–1189, 2010
Aydin S, Kucukyuruk B, Abuzayed B, Aydin S, Sanus GZ: Cranioplasty: review of materials and techniques. J Neurosci Rural Pract 2(2): 162–167, 2011
Bhakta G, Ekaputra AK, Rai B, Abbah SA, Tan TC, Le BQ, et al: Fabrication of polycaprolactone-silanated beta-tricalcium phosphate-heparan sulfate scaffolds for spinal fusion applications. Spine J 18(5): 818–830, 2018
Biasibetti A, Aloj D, Di Gregorio G, Masse A, Salomone C: Mechanical and biological treatment of long bone non-unions. Injury 36(Suppl. 4): S45–S50, 2005
Bosch C, Melsen B, Vargervik K: Importance of the critical-size bone defect in testing bone-regenerating materials. J Craniofac Surg 9(4): 310–316, 1998
Bramono DS, Murali S, Rai B, Ling L, Poh WT, Lim ZX, et al: Bone marrow-derived heparan sulfate potentiates the osteogenic activity of bone morphogenetic protein-2 (BMP-2). Bone 50(4): 954–964, 2012
Colombier ML, Lafont J, Blanquaert F, Caruelle JP, Barritault D, Saffar JL: A single low dose of RGTA, a new healing agent, hastens wound maturation and enhances bone deposition in rat craniotomy defects. Cells Tissues Organs 164(3): 131–140, 1999
Cool SM, Nurcombe V: Heparan sulfate regulation of progenitor cell fate. J Cell Biochem 99(4): 1040–1051, 2006
Donati D, Zolezzi C, Tomba P, Vigano A: Bone grafting: historical and conceptual review, starting with an old manuscript by Vittorio Putti. Acta Orthop 78(1): 19–25, 2007
Escartin Q, Lallam-Laroye C, Baroukh B, Morvan FO, Caruelle JP, Godeau G, et al: A new approach to treat tissue destruction in periodontitis with chemically modified dextran polymers. FASEB J 17(6): 644–651, 2003
Feroze AH, Walmsley GG, Choudhri O, Lorenz HP, Grant GA, Edwards MS: Evolution of cranioplasty techniques in neurosurgery: historical review, pediatric considerations, and current trends. J Neurosurg 123(4): 1098–1107, 2015
He X, Liu Y, Yuan X, Lu L: Enhanced healing of rat calvarial defects with MSCs loaded on BMP-2 releasing chitosan/alginate/hydroxyapatite scaffolds. PLoS One 9(8): e104061, 2014
Herford AS, Stoffella E, Tandon R: Reconstruction of mandibular defects using bone morphogenic protein: can growth factors replace the need for autologous bone grafts? A systematic review of the literature. Plast Surg Int 2011: 165824, 2011
Jackson RA, Murali S, van Wijnen AJ, Stein GS, Nurcombe V, Cool SM: Heparan sulfate regulates the anabolic activity of MC3T3-E1 preosteoblast cells by induction of Runx2. J Cell Physiol 210(1): 38–50, 2007
Khader BA, Towler MR: Materials and techniques used in cranioplasty fixation: a review. Mater Sci Eng C Mater Biol Appl 66: 315–322, 2016
Krishnan P, Kartikueyan R, Roychowdhury S: Near-total bone flap resorption following autologous bone cranioplasty in a child. Pediatr Neurosurg 51(2): 109–110, 2016
Lafont J, Baroukh B, Berdal A, Colombier ML, Barritault D, Caruelle JP, et al: RGTA11, a new healing agent, triggers developmental events during healing of craniotomy defects in adult rats. Growth Factor 16(1): 23–38, 1998
Lee L, Ker J, Quah BL, Chou N, Choy D, Yeo TT: A retrospective analysis and review of an institution's experience with the complications of cranioplasty. Br J Neurosurg 27(5): 629–635, 2013
Lee SH, Yoo CJ, Lee U, Park CW, Lee SG, Kim WK: Resorption of autogenous bone graft in cranioplasty: resorption and reintegration failure. Korean J Neurotrauma 10(1): 10–14, 2014
Lee SS, Fyrner T, Chen F, Alvarez Z, Sleep E, Chun DS, et al: Sulfated glycopeptide nanostructures for multipotent protein activation. Nat Nanotechnol 12(8): 821–829, 2017
Li Y, Wu Z-g, Li X-k, Guo Z, Wu S-h, Zhang Y-q, et al: A polycaprolactone-tricalcium phosphate composite scaffold as an autograft-free spinal fusion cage in a sheep model. Biomaterials 35(22): 5647–5659, 2014
Ling L, Murali S, Dombrowski C, Haupt LM, Stein GS, van Wijnen AJ, et al: Sulfated glycosaminoglycans mediate the effects of FGF2 on the osteogenic potential of rat calvarial osteoprogenitor cells. J Cell Physiol 209(3): 811–825, 2006
Ling L, Murali S, Stein GS, van Wijnen AJ, Cool SM: Glycosaminoglycans modulate RANKL-induced osteoclastogenesis. J Cell Biochem 109(6): 1222–1231, 2010
Manton KJ, Sadasivam M, Cool SM, Nurcombe V: Bone-specific heparan sulfates induce osteoblast growth arrest and downregulation of retinoblastoma protein. J Cell Physiol 209(1): 219–229, 2006
Martin KD, Franz B, Kirsch M, Polanski W, von der Hagen M, Schackert G, et al: Autologous bone flap cranioplasty following decompressive craniectomy is combined with a high complication rate in pediatric traumatic brain injury patients. Acta Neurochir (Wien) 156(4): 813–824, 2014
Maus U, Andereya S, Gravius S, Ohnsorge JA, Niedhart C, Siebert CH: BMP-2 incorporated in a tricalcium phosphate bone substitute enhances bone remodeling in sheep. J Biomater Appl 22(6): 559–576, 2008
Morina A, Kelmendi F, Morina Q, Dragusha S, Ahmeti F, Morina D, et al: Cranioplasty with subcutaneously preserved autologous bone grafts in abdominal wall-experience with 75 cases in a post-war country Kosova. Surg Neurol Int 2: 72, 2011
Motamedian SR, Hosseinpour S, Ahsaie MG, Khojasteh A: Smart scaffolds in bone tissue engineering: a systematic review of literature. World J Stem Cells 7(3): 657–668, 2015
Murali S, Manton KJ, Tjong V, Su X, Haupt LM, Cool SM, et al: Purification and characterization of heparan sulfate from human primary osteoblasts. J Cell Biochem 108(5): 1132–1142, 2009
Murali S, Rai B, Dombrowski C, Lee JL, Lim ZX, Bramono DS, et al: Affinity-selected heparan sulfate for bone repair. Biomaterials 34(22): 5594–5605, 2013
Pape HC, Evans A, Kobbe P: Autologous bone graft: properties and techniques. J Orthop Trauma 24(Suppl. 1): S36–S40, 2010
Park SP, Kim JH, Kang HI, Kim DR, Moon BG, Kim JS: Bone flap resorption following cranioplasty with autologous bone: quantitative measurement of bone flap resorption and predictive factors. J Korean Neurosurg Soc 60(6): 749–754, 2017
Rai B, Chatterjea A, Lim ZXH, Tan TC, Sawyer AA, Hosaka YZ, et al: Repair of segmental ulna defects using a beta-TCP implant in combination with a heparan sulfate glycosaminoglycan variant. Acta Biomater 28: 193–204, 2015
Rai B, Ho KH, Lei Y, Si-Hoe KM, Jeremy Teo CM, Yacob KB, et al: Polycaprolactone-20% tricalcium phosphate scaffolds in combination with platelet-rich plasma

for the treatment of critical-sized defects of the mandible: a pilot study. J Oral Maxillofac Surg 65(11): 2195–2205, 2007a
Rai B, Oest ME, Dupont KM, Ho KH, Teoh SH, Guldberg RE: Combination of platelet-rich plasma with polycaprolactone-tricalcium phosphate scaffolds for segmental bone defect repair. J Biomed Mater Res A 81(4): 888–899, 2007b
Rai B, Teoh SH, Ho KH, Hutmacher DW, Cao T, Chen F, et al: The effect of rhBMP-2 on canine osteoblasts seeded onto 3D bioactive polycaprolactone scaffolds. Biomaterials 25(24): 5499–5506, 2004
Rai B, Teoh SH, Hutmacher DW, Cao T, Ho KH: Novel PCL-based honeycomb scaffolds as drug delivery systems for rhBMP-2. Biomaterials 26(17): 3739–3748, 2005
Sakkas A, Wilde F, Heufelder M, Winter K, Schramm A: Autogenous bone grafts in oral implantology-is it still a "gold standard"? A consecutive review of 279 patients with 456 clinical procedures. Int J Implant Dent 3(1): 23, 2017
Samsonraj RM, Dudakovic A, Zan P, Pichurin O, Cool SM, van Wijnen AJ: A Versatile protocol for studying calvarial bone defect healing in a mouse model. Tissue Eng C Methods 23(11): 686–693, 2017
Sawyer AA, Song SJ, Susanto E, Chuan P, Lam CX, Woodruff MA, et al: The stimulation of healing within a rat calvarial defect by mPCL-TCP/collagen scaffolds loaded with rhBMP-2. Biomaterials 30(13): 2479–2488, 2009
Shah MM, Smyth MD, Woo AS: Adverse facial edema associated with off-label use of recombinant human bone morphogenetic protein-2 in cranial reconstruction for craniosynostosis. Case report. J Neurosurg Pediatr 1(3): 255–257, 2008
Shim JH, Won JY, Park JH, Bae JH, Ahn G, Kim CH, et al: Effects of 3D-printed polycaprolactone/beta-tricalcium phosphate membranes on guided bone regeneration. Int J Mol Sci 18(5), 2017
Song SJ, Hutmacher D, Nurcombe V, Cool SM: Temporal expression of proteoglycans in the rat limb during bone healing. Gene 379: 92–100, 2006
Sundseth J, Sundseth A, Berg-Johnsen J, Sorteberg W, Lindegaard KF: Cranioplasty with autologous cryopreserved bone after decompressive craniectomy: complications and risk factors for developing surgical site infection. Acta Neurochir (Wien) 156(4): 805–811, 2014 discussion 811
Woodruff MA, Rath SN, Susanto E, Haupt LM, Hutmacher DW, Nurcombe V, et al: Sustained release and osteogenic potential of heparan sulfate-doped fibrin glue scaffolds within a rat cranial model. J Mol Histol 38(5): 425–433, 2007
Yang HS, La WG, Cho YM, Shin W, Yeo GD, Kim BS: Comparison between heparin-conjugated fibrin and collagen sponge as bone morphogenetic protein-2 carriers for bone regeneration. Exp Mol Med 44(5): 350–355, 2012
Yeo A, Cheok C, Teoh S, Zhang Z, Buser D, Bosshardt D: Lateral ridge augmentation using a PCL-TCP scaffold in a clinically relevant but challenging micropig model. Clin Oral Implant Res 23(12): 1322–1332, 2012
Yeo A, Rai B, Sju E, Cheong JJ, Teoh SH: The degradation profile of novel, bioresorbable PCL-TCP scaffolds: an in vitro and in vivo study. J Biomed Mater Res A 84(1): 208–218, 2008
Yeo A, Wong WJ, Khoo HH, Teoh SH: Surface modification of PCL-TCP scaffolds improve interfacial mechanical interlock and enhance early bone formation: an in vitro and in vivo characterization. J Biomed Mater Res A 92(1): 311–321, 2010a
Yeo A, Wong WJ, Teoh SH: Surface modification of PCL-TCP scaffolds in rabbit calvaria defects: evaluation of scaffold degradation profile, biomechanical properties and bone healing patterns. J Biomed Mater Res A 93(4): 1358–1367, 2010b
Zanotti B, Zingaretti N, Verlicchi A, Robiony M, Alfieri A, Parodi PC: Cranioplasty: review of materials. J Craniofac Surg 27(8): 2061–2072, 2016
Zein I, Hutmacher DW, Tan KC, Teoh SH: Fused deposition modeling of novel scaffold architectures for tissue engineering applications. Biomaterials 23(4): 1169–1185, 2002